Albaydha University Journal – Vol.(5)-Issue(4) 2023(special Issue of the Fourth Scientific Conference of Albaydha University)

The inhibition of 3H-2- Methyl-1,2,4-Triazepino[2,3-a] Benzimidazole-4(5h)-one (MTB) on corrosion of mild steel in 1 M HCl solutions; Theatrical and experimental study

A. Al Maofari[1,2*], A. SABER[3], K. Al maamar[3], N. Labjar[4], E.M. Essassi[3], S. El Hajjaji[1]

[1]Laboratory of Spectroscopy, Molecular Modeling, Materials and Environment, Faculty of Sciences, University Mohamed V, Morocco

[2]Laboratory of Analytical /Physical Chemistry, Department of Chemistry, Faculty of Sciences, Sa'adah University, Yemen

[3]Laboratory of Heterocyclic Organic Chemistry, Faculty of Sciences, University Mohamed V, Morocco

[4]Laboratory of Mechanics, and Industrial process, Chemical Sciences Research Team, ENSET, Mohamed V University in Rabat E-10100, Morocco

*Corresponding author, E-mail: mofary66@yahoo.com

DOI: https://doi.org/10.56807/buj.v5i4.472

Abstract

The inhibitive action of a new Benzimidazole derivation, 3H-2-Methyl-1,2,4-Triazepino [2,3-a] Benzimidazole-4 (5h)-one (MTB), for the corrosion of mild steel in one molar hydrochloric acid solution was investigated. Corrosion tests has been conducted using weight loss measurement electrochemical method and scanning electron microscopy associated with energy dispersion spectrometer (SEM/EDS). The results showed increasing inhibition efficiency with increasing the inhibitor concentration and reach to 98% at 1×10^{-2} M. The thermal studies indicated that the newly synthesized MTB inhibited the corrosion of mild steel by its adsorbing on the specimen surface via both physisorption and chemisorption mechanism. The adsorption process of MTB on the mild steel surface obeys Langmuir adsorption isotherm and act as mix-type inhibitor. The analysis of surface morphology confirmed the thermal results by showing the MTB molecules on the mild steel surface. Various DFT parameter like HOMO and LUMO energy, gab energy (ΔE), electronegativity (χ), softness (σ), global hardness (η) were derived for MTB molecules and correlated with experimental results.

Keywords: *Surface morphology, Thermal study, Corrosion, Inhibitor, Polarization, Mild Steel, Isotherm, Benzimidazole, Quantum chemical, DFT Calculation.*

1. Introduction

Acid solutions are extensively used in a variety of industrial processes such as oil well acidification, acid pickling and acidic cleaning [1, 2], which generally lead to serious metallic corrosion. The addition of inhibitors is one of the most practical methods of corrosion protection. Among them, heterocyclic organic compounds containing sulfur, phosphorus, oxygen, nitrogen and aromatic rings are the most effective and efficient inhibitors for the metals in acidic medium due to their special molecular structure [3–9]. In many factors for the inhibiting effects, the planarity of heterocycles and the presence of lone pair of electrons on heterocyclic atoms are particularly important structure characteristics because they mainly determine the adsorption of inhibitor molecules on metal surface [10–12]. On the other hand, the surface state and excess charge of the metal surface also affect the adsorption behaviour of inhibitor molecule on metal surface [13,14]. Generally, the tendency to form a stronger coordination bond, and consequently resulting in the high inhibition efficiency, increases in the following order O < N < S < Se < P [15-18]. Nitrogen containing organic compounds have been found to act as good corrosion inhibitors and their inhibition mechanism has been illustrated in terms of the number of lone electron pairs, the π orbital character of free electrons and the electron density around the nitrogen atom [4, 19–23]. In recent years, benzimidazole and its derivatives have been received considerable attention on their inhibition properties for metallic corrosion and demonstrated that they are excellent inhibitors for metals and alloys in acidic solution since the nitrogen atom and the aromatic ring in molecular structure are likely to facilitate the adsorption of compounds on the metallic surface [24–33].To characterize the adsorbed layer and the interaction between adsorbed species, adsorption isotherms are used. The following adsorption isotherms are the most common models to study the mechanism of corrosion inhibition [34–38]:

Langmuir adsorption isotherm:

$$\theta = \frac{KC_{inh}}{1+KC_{inh}} \qquad (1)$$

Temkin adsorption isotherm:

$$\exp(-2a\theta) = KC_{inh} \qquad (2)$$

Frumkin adsorption isotherm:

$$(\frac{\theta}{1-\theta})\exp(-2a\theta) = KC_{inh} \qquad (3)$$

In the above, C is the concentration of inhibitor, *k* the adsorption constant and θ the surface coverage. The parameter «a» in Temkin isotherms is called “surface heterogeneity” and “interaction parameter Frumkin adsorption. Different methods including weight loss measurement, electrochemical AC and DC methods or combination of these methods have been used to determine surface coverage (θ) and the adsorption isotherms of inhibitor molecules in the corrosive media [38].

The aim of this work was to study the interaction mechanism between the inhibitor molecules and the mild steel surface inhibition, the corrosion inhibition performances of MTB at various concentrations for mild steel in 1M HCl solution were investigated by weight loss and potentiodynamic polarization measurement, which were confirmed by surface morphology analysis using scanning electron microscopy associated with energy dispersion spectrometer (SEM/EDS). This work also completed with chemical calculations which used to provide a clear understanding of the interfacial adsorption process of MTB on mild steel surface.

2.Experimental

2.1. Materials and chemicals.

The corrosion tests were performed on mild steel samples with a composition (wt.%): C, 0.370; Mn, 0.680; Si, 0.230; S, 0.0016; Cr, 0.077; Ti, 0.011; Ni, 0.059; Co, 0.009; Cu, 0.160 and Fe balance. The specimens were used for weight loss test were in the rectangular shape with dimensions 1×1×0.15 cm. For electrochemical measurements, except the exposed working surface (1 cm^2), the remainder of working electrode was embedded in epoxy. Prior to experiments, all of the specimens and electrodes were gradually abraded with SiC papers up to 800 grit, followed by cleaning with bi-distilled water and degreasing with acetone, and finally dried with cool air and stored in a vacuum desiccator.

The employed concentrations of the inhibitors were varied from 10.0 to 0.1 mM. All the test solutions were prepared from analytical-grade chemical reagents in distilled water without further purification. For each experiment, a freshly prepared solution was used. The test solutions were opened to the atmosphere and the temperature was controlled thermostatically. The studied structures of 3H-2-Methyl-1,2,4-Triazepino[2,3-a] Benzimidazole-4(5h)-one(MTB) is presented below:

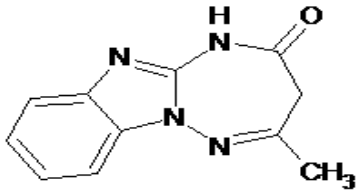

Figure 1: Molecular structure of the 3H-2- Methyl-1,2,4- Triazepino [2,3-a] Benzimidazole-4(5h)-one (MTB)

2.2. Weight loss measurements

A determined surface area ($S\ cm^2$) of mild steel specimens were polished with different grades of sand papers, washed with bi-distilled water, dried and kept in a desiccator. After weighting accurately (m_{Int}) by a digital balance with sensitivity of 0.1 mg the specimens were immersed in solution containing 1 M HCl solution without and with inhibitor at 0.01M. After one week and everyday exposure (immersing time; t_{im}), the specimens were taken out rinsed thoroughly with distilled water, dried and weighted accurately again (m_{Fin}). Weight loss allowed calculation of inhibition efficiency (IE%) of our inhibitor according to the following equations:

$$W = \frac{m_{Int} - m_{Fin}}{S \times t_{im}} \qquad (4)$$

$$IE(\%) = \frac{W - W_{inh}}{W} \times 100 \qquad (5)$$

Where W and W_{inh} are the corrosion rate of mild steel samples obtained in HCl 1M solution in the absence and in the presence of inhibitor, respectively.

2.3 Polarization measurements

Electrochemical measurements were carried out in a conventional three electrode cylindrical glass cell, containing 100 ml of electrolyte at the temperature controlled thermostatically. All potentials were reported vs. the saturated calomel electrode (SCE); Platinum electrode was used as a counter electrode (CE). The Potentiodynamic curves of mild steel in HCl 1M solution in the absence and in the presence of MTB were obtained with potential range from-1 to +0.2 V. For polarization measurements, a potentiostat Voltalab 301 PGZ monitored by a PC computer and Voltamaster 4.0 software were used for run the tests, collect and evaluate the experimental data. During each experiment, the test solution was mixed with a magnetic stirrer.

The degree of surface coverage (θ) and the percentage of inhibition efficiency (IE %) were calculated using the following equations:

$$IE(\%) = \frac{I_{corr} - I_{corr(inh)}}{I_{corr}} \times 100 \quad (6)$$

$$\theta = \frac{I_{corr} - I_{corr(inh)}}{I_{corr}} \quad (7)$$

Where I_{corr} and $I_{corr(inh)}$ are, respectively, the corrosion current densities obtained in HCl 1M solution in the absence and the presence of inhibitor.

3. Results and discussion

3.1. Potentiodynamic polarization results

Fig. 2 shows the cathodic and anodic polarization plots of mild steel immersed in 1M HCl solution at room temperature in absence and presence of different concentrations of MTB. The corrosion current density was calculated from the intersection of cathodic and anodic Tafel line.

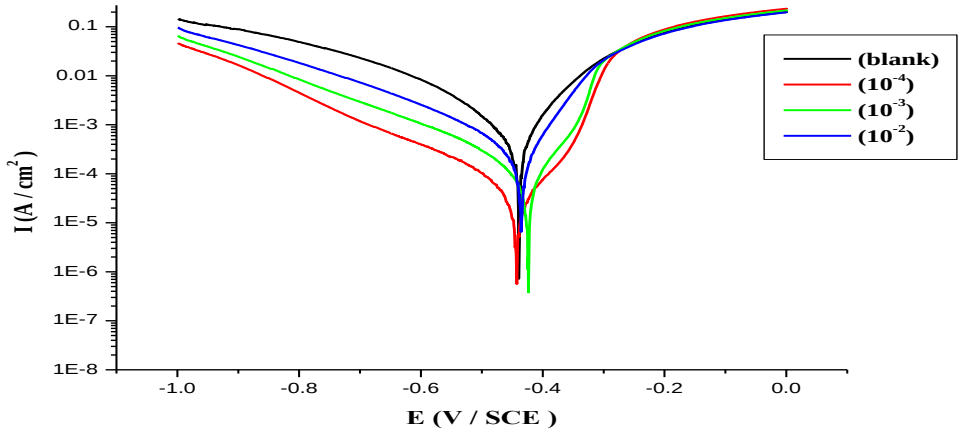

Figure 2: Anodic and cathodic polarization curves (Tafel curves) for mild steel in 1M HCl without and with various concentration of inhibitor at room temperature.

The values of the electrochemical parameters for the different MTB concentrations are given in Table 1. The data show that the increasing of MTB concentration decreases the corrosion current density (I_{corr}) and consequently the inhibition efficiency of MTB increased. The presence of inhibitor resulted in a shift of the corrosion potential (Ecorr) toward more negative values by 60-80 mV in comparison to the result obtained in the absence of inhibitor. The inhibition efficiency was estimated to be 98%for MTB at 10^{-2} M, and act as mix-type inhibitor.

Table 1: Electrochemical parameters of mild steel at various concentrations of MTB in 1M HCl at room temperature.

$C_{inh}(M)$	$I_{corr}(mA/cm^2)$	$E_{corr}mV/ECS$	θ	IE%
Blank	3.845	-438	-	-
10^{-4}	0.442	-434	0.8850	88.5
10^{-3}	0.145	-421	0.9623	96.23
10^{-2}	0.066	-443	0.9828	98.28

3.2. Adsorption isotherms

Adsorption isotherms provide information about the interaction of the adsorbed molecules on the electrode surface [39,40]. The adsorption of an organic adsorbate at metal–solution interface can be

presented as a substitution adsorption process between the organic molecules in aqueous solution, (Org_{sol}), and thewater molecules on metallic surface, (H_2O_{ads}) [40]:

$$Org_{sol} + xH_2O_{ads} \Leftrightarrow Org_{ads} + H_2O_{sol}$$

where Org_{sol} and Org_{ads} are the organic specie dissolved in the aqueous solution and adsorbed onto the metallic surface, respectively,H_2O_{ads} is the water molecule adsorbed on the metallic surface and x is the size ratio representing the number of water molecules replaced by one organic adsorbed. For the studied inhibitors, it was found that the experimental data obtained from polarization readings could be fitted by Langmuir's adsorption isotherm. According to this isotherm, the surface coverage (θ) is related to inhibitor concentration (C). The Langmuir's linear equation (Eq. 8) gives from the equation 1 Rearrangement as follows.

$$\frac{\theta}{1-\theta} = k_{ads} \times C \qquad (7)$$

:

$$\frac{C_{inh}}{\theta} = \frac{1}{k_{ads}} + C_{inh} \qquad (8)$$

Where k_{ads} is the equilibrium constant of the inhibitor adsorption process, C is the inhibitor concentration and θ is the surface coverage that was calculated by Eq. 6. This model for Langmuir's adsorption isotherm has been used extensively in the literatures for various metal/inhibitor/acid solution systems [39 - 42]. A fitted straight line is obtained for the plot of C/θ versus C with slopes close to 1 as seen in Fig. 3. The strong correlation (R^2> 0.99) suggests that the adsorption of inhibitor on the mild steel surface obeyed this isotherm. This isotherm assumes that the adsorbed molecules occupy only one site and there are no interactions with other adsorbed species [41].

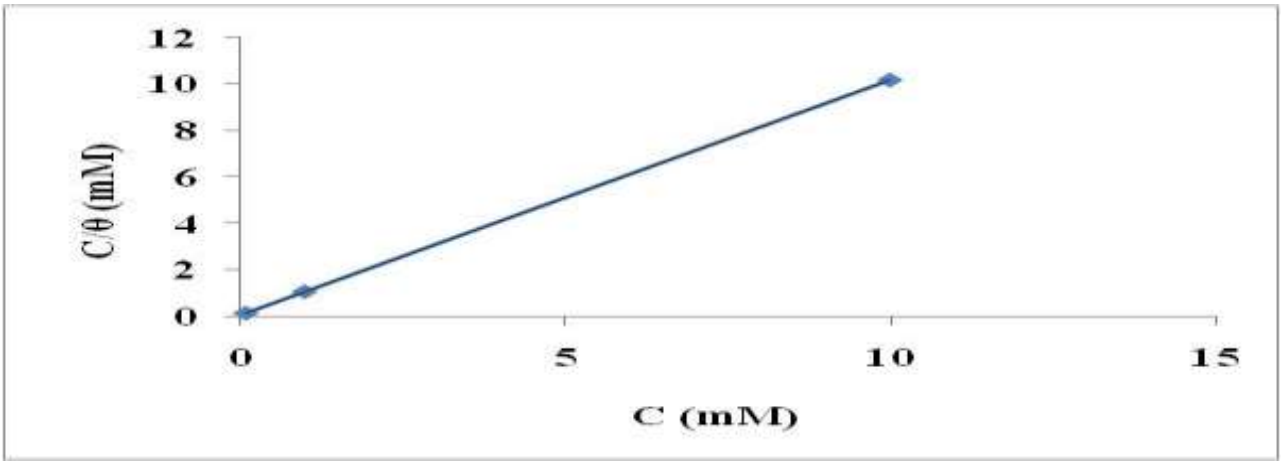

Figure 3: Langmuir adsorption isotherm (C/θ vs. C) of inhibitors in 1M HCl at room temperature.

The k_{ads} values can be calculated from the intercept lines on the C/θ-axis. This is related to the standard free energy of adsorption ΔG_{ads} with the following equation:

$$K_{ads} = \frac{1}{55.5} e^{\left(\frac{-\Delta G_{ads}}{RT}\right)} \qquad (9)$$

Where R is the gas constant and T is the absolute temperature. The constant value of 55.5 is the concentration of water in solution. The negative sign of ΔG_{ads} indicate thatthe inhibitors are spontaneously adsorbed onto the metal surface[41,42]. Generally, the magnitude of ΔG_{ads}around -20 kJ/mol or less negative is assumed for electrostatic interactions exist between inhibitor and the charged metal surface (physisorption). Those around -40 kJ/mol or more negative are indicating of charge sharing or transferring from organic specie to the metal surface to form a coordinate type of metal bond

(chemisorption) [41-44]. In some literatures, the values of ΔG_{ads} are reported less negative than -40 kJ/mol for physical adsorption commonly interpreted as the formation of an adsorptive film with an electrostatic character [46, 47]. The calculated value of free energy of adsorption for MTB was found to be -34.89kJ/mol, this value suggests that the adsorption mechanism of MTB onto the steel surface involves two types of interaction physisorption and chemisorption. The higher inhibition effects of MTB may be attributed to the presence of nitrogen atoms, at the same time in its molecular structure [42,44].

3.3 Effect of temperature

The effect of temperature on the inhibited acid-metal reaction is very complex, because many changes occur on the metal surface such as rapid etching and desorption of inhibitor and the inhibitor itself may undergo decomposition [48]. The change of the corrosion rate with the temperature was studied in 1M HCl, both in absence and presence of MTB. For this purpose, polarization readings were performed at different temperatures from 25°C to 55°C in absence and presence of MTB (Fig. 4). The electrochemical parameters were extracted and summarized in Table 2. Corrosion inhibition efficiencies (98 %) calculated from Eq. 5 are also shown in Table 4.

Fig. 4A and 4B show that raising the temperature shifts corrosion potentials to nobler potentials, this led to a higher corrosion rate (I_{corr}). The value of E_{corr} is also shifted toward the noble direction by the presence of inhibitors. The inhibition efficiencies for MTB are decreased with temperature which is a characteristic of the physical adsorption [49].

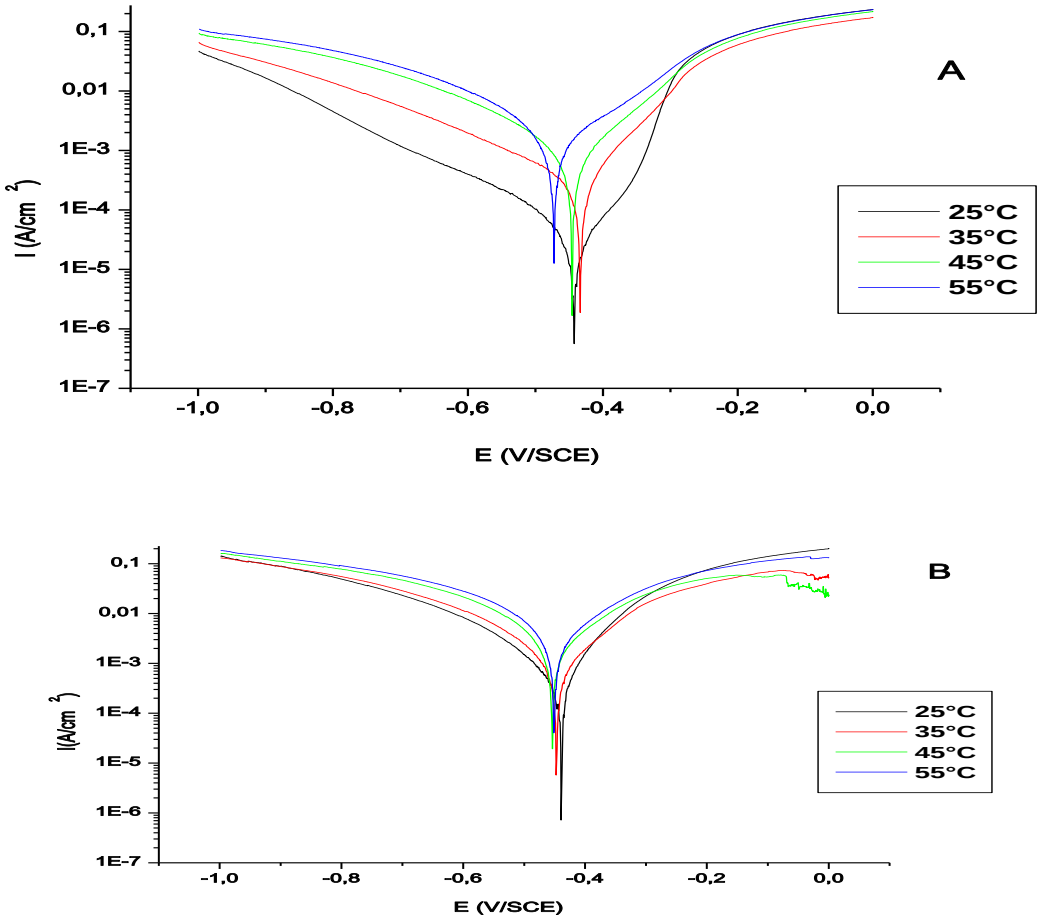

Figure 4: Effect of temperature on the cathodic and anodic responses for C38 steel in 1M HCl (A) and 1MHCl + 0.1M of MTB (B).

Table 2: Electrochemical parameters and the corresponding inhibition efficiencies at various temperatures studied of mild steel in 1M HCl containing 0.01M of MTB.

T(°C)	BLANK		Inhibitor (MTB)		
	I_{corr} (mA/cm^2)	E_{corr} (mV/SCE)	I_{corr} (mA/cm^2)	E_{corr} (mV/SCE)	IE%
25	2.8	-445	0.066	-433	98
35	5.21	-448	0.32	-435	94
45	10	-451	1.1	-440	89
55	20	-454	6.3	-474	68

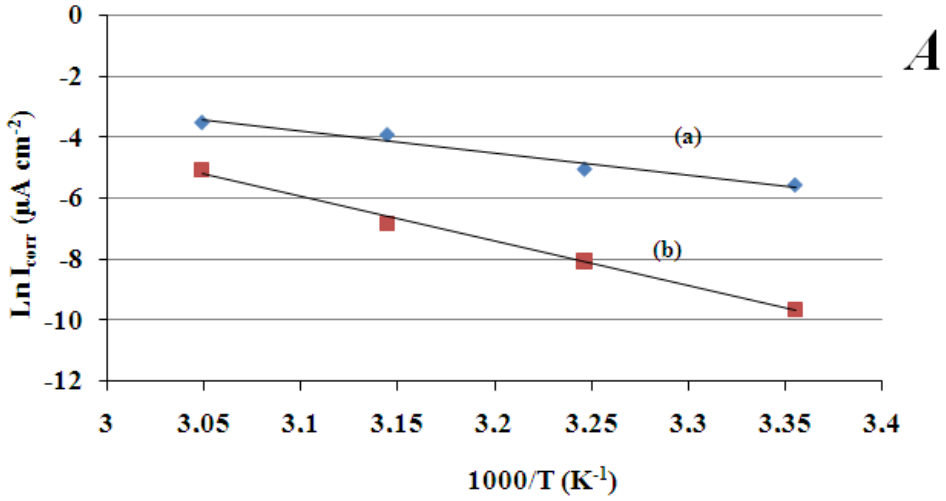

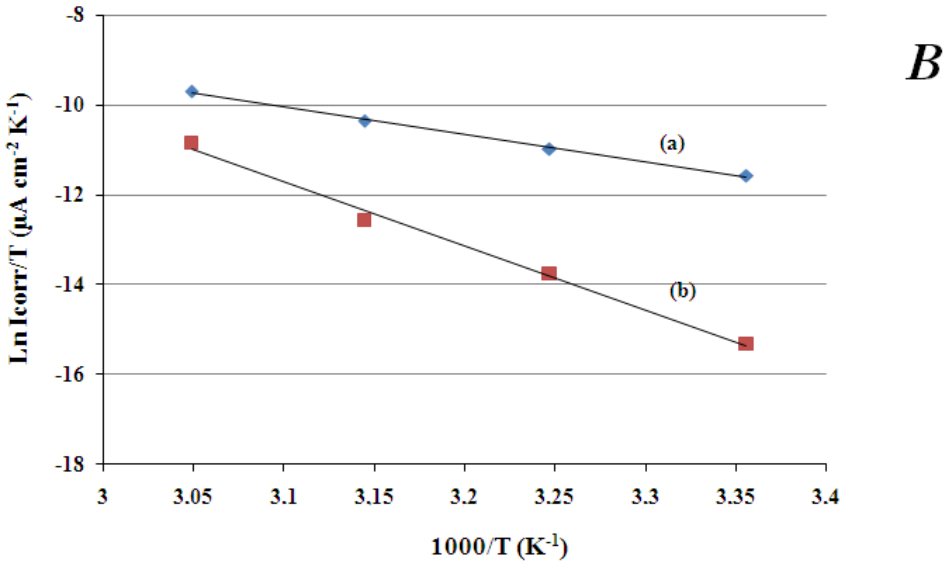

Figure 5A and 5B: The Arrhenius plots of Ln I_{corr} and Ln (Icorr/T) against (1000/T), for mild steel dissolution in 1M HCl in the absence (a) and presence (b) of 0.01M of MTB.

According to the Arrhenius equation, the apparent activation energy (E_a) of metal corrosion in both media (blank and inhibited) can be calculated from the following equations:

$$lnI_{corr} = \ln k - \left(\frac{E_a}{RT}\right) \qquad (10)$$

Where *k* is the Arrhenius pre-exponential constant. Fig. 5A shows the plots of logarithm I_{corr} against the reciprocal of temperature in the absence and presence of MTB. The slopes of the lines are $-E_a/R$ which are extracted and shown in Table 3. The calculated value of E_a in the absence of inhibitor is 53.16 kJ/mol, while in the presence of MTB is 121.02. In the literatures, the higher E_a for corrosion process in the presence of an inhibitor is attributed to the physisorption of inhibitor [50, 51]. The enthalpy of activation (ΔH_a°) and the entropy of activation (ΔS_a°) for the corrosion of mild steel in HCl were obtained by applying the transition-state equation.

$$\ln\frac{I_{corr}}{T} = \left(\ln\frac{R}{Nh} + \frac{\Delta S_a^\circ}{R}\right) - \frac{\Delta H_a^\circ}{RT} \qquad (11)$$

Fig.5B shows the plots of logarithm I_{corr}/T against the reciprocal of temperature in the absence and presence of MTB. The slopes of the lines are $\frac{\Delta H_a^\circ}{R}$ which are extracted and shown in Table 3.

Table 3: Thermodynamic and equilibrium adsorption parameters for adsorption MTB on mild steel surface in 1M HCl solutions.

Inhibitor	**E_a (kJ/mol)**	**ΔH_{ads}^0(kJ/mol)**	**ΔS_{ads}^0(J/mol)**
Blank	53.16	50.56	-124,41
MTB(10^{-2} M)	121.02	118.42	70.42

The values of thermodynamic parameters (ΔH_a° and ΔS_a°) for the adsorption of inhibitors can provide valuable information about the mechanism of corrosion inhibition. While an endothermic adsorption process ($\Delta H_a^\circ > 0$) is attributed unequivocally to chemisorption, an exothermic adsorption process ($\Delta H_a^\circ < 0$) may involve physisorption, chemisorption or a mixture of both [47-50]. In an exothermic process, physisorption can be distinguished from chemisorption. Moreover, the large value of enthalpies in

presence of MTB compared with blank solution mean more energy barrier is needed for mild steel dissolution (the inhibitor increases the corrosion resistance of mild steel).

The positive sign of ΔS_a° is also related to substitutional process, which can be attributed to the increase in the solvent entropy and more positive water desorption entropy [45, 52]. It also interpreted with increase of disorders due to the more water molecules which can be desorbed from the metal surface by one inhibitor molecule [45,46].

3.4. Weight loss measurements

The corrosion rate and inhibition efficiency in mild steel alloy in 1M HCl solution at room temperature in absence and presence of MTB were given in Table 4. It is evident from these results that inhibition efficiency of mild steel alloy in 1M HCl solution containing 10^{-2} M (MTB) at room temperature is 93%.

Table 4: Corrosion parameters obtained from weight loss measurements of mild steel alloy in HCl solution containing 10^{-2} M (MTB) at room temperature

Time in (h)	V without inhibitor ($mgh^{-1}cm^{-2}$)	V with inhibitor ($mgh^{-1}cm^{-2}$)	IE (%)
22	0.020	0.0053	73.5
66	0.020	0.0035	82.5
88	0.023	0.0026	88.7
110	0.025	0.0021	91.6
132	0.025	0.0018	92.8
154	0.024	0.0015	93.8

3.5. SEM-EDS Examination

To investigate the performance of the inhibitor, an SEM study of mild steel was carried out after 168h exposure test at free potential in 1M HCl solution with and without MTB. Before immersion, mild steel characterized by SEM (Fig.6). There is thus a complex metallurgical structure, containing different phases, as can be seen in the micrograph of fig. 6. After immersion in 1M HCl media in absence and presence of MTB, the presence of corrosion products on the surface was noticed. In the absence of inhibitor, the structure of the alloy is still observed and a thick and discontinuous corrosion product layer was observed, EDS analysis shows the presence of oxygen. Contrarily, in the presence of MTB, the surface was covered by a continuous and uniform layer, EDS analysis shows the presence of nitrogen this indicated to MTB adsorption on steel surface.

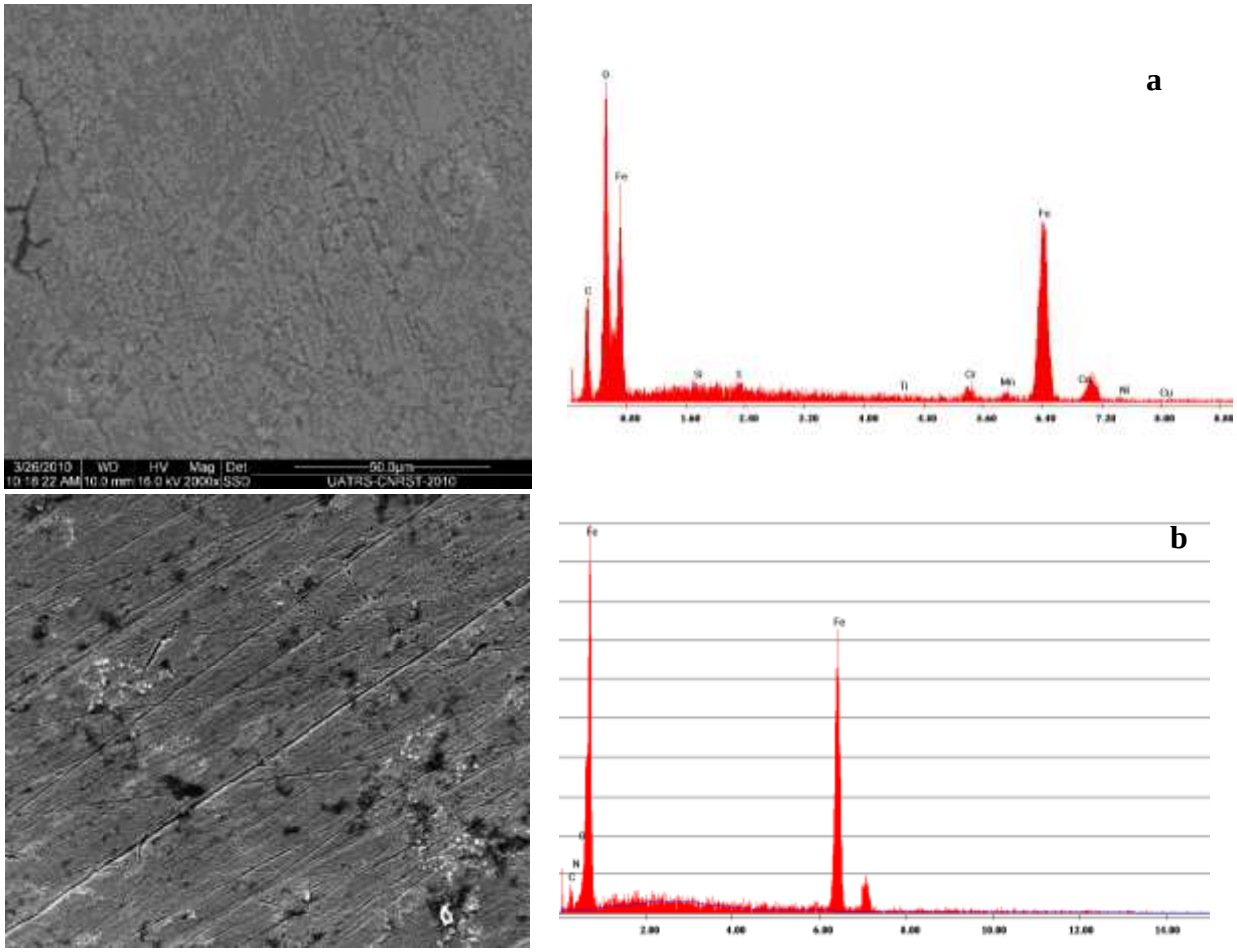

Figure 6: SEM micrographs of the surface of mild steel before and after immersion in 1M HCl solution: After immersion (a) in the absence of inhibitor (b) in presence of inhibitor.

3.6. The Results of DFT Study.

The mode of adsorption of MTB on mild steel surface was studied utilizing the density function theory (DFT) with the Beck's three parameter exchange functional along with the Lee–Yang–Parr nonlocal correlation functional (B3LYP) complemented with basis set with 6-31G +(d,p) that was carried out on GausView 06 interface and Gaussian 09 [57–59]. The quantum approach was used to figure some quantum parameters, for example, lowest unoccupied molecular orbital energy (E LUMO), high occupied molecular orbital energy(E HOMO), energy of gap (ΔE), chemical potential (μ), ionization potential (I) electron affinity (A), chemical softness (σ), chemical hardness (η), Electrophilicity index (ω), Electroappcepting-power (ω+), Electrodonating-power (ω-), net electrophilicity (Δω±), Back-donation Energy ($\Delta E_{B.D}$) and electronegativity (global electronic chemical potential; χ))by using the following equations [59-61]

$$I = -E_{HOMO} \quad (12)$$

$$A = -E_{LUMO} \quad (13)$$

$$\Delta E = E_{LUMO} - E_{HOMO} \quad (14)$$

$$\eta = \frac{1}{2}(E_{LUMO} - E_{HOMO}) \quad (15)$$

$$\sigma = \frac{1}{\eta} \quad (16)$$

$$\chi = \frac{1}{2}(-E_{HOMO} - E_{LUMO}) \quad (17)$$

$$\mu = -\chi = \frac{1}{2}(E_{HOMO} + E_{LUMO}) \quad (18)$$

$$\omega = \frac{\mu^2}{2\eta} \quad (19)$$

$$\omega^+ = \frac{(-3E_{LUMO}-E_{HOMO})^2}{16\times(E_{LUMO}-E_{HOMO})} \quad (20)$$

$$\omega^- = \frac{(-E_{LUMO}-3E_{HOMO})^2}{16\times(E_{LUMO}-E_{HOMO})} \quad (21)$$

$$\Delta\omega^{\pm} = \omega^+ + \omega^- \quad (22)$$

$$\Delta E_{Back\ Donation} = -\frac{\eta}{4} \quad (23)$$

The calculated quantum chemical parameters of MTB related to the most stable confirmation of molecule electronic structure are shown in Table 5.

Table 5. Electronic and structural parameters for MTB molecule employing DFT approach.

Theoretical parameters	MTB
E_{LUMO} (eV)	-0.899
E_{HOMO} (eV)	-6.02
ΔE (eV)	8.08
Ionization energy (I) eV	6.02
Electron affinity (A) eV	0.899
Electronegativity (χ) eV	3.46
Chemical softness (σ) eV^{-1}	0.39
Chemical hardness (η) eV	2.56
Electrophilicity (ω) eV	2.34
Chemical potential (μ) eV	-3.46
Electroappcepting-power ω^+ (eV)	0.93
Electrodonating-power ω^- (eV)	4.38
Net electrophilicity $\omega^{\pm}$ (eV)	5.31
Back-donation Energy $\Delta E_{B.D}$(eV)	-0.64
D. Moment (Debey)	2.73

A high value of global electronegativity (χ) suggests that undertaken compound is less potent to donate/ transfer its electron to the appropriate acceptor molecule e.g. d-orbital of the surface Fe atoms in the present case. As The mediated value of (χ) for MTB indicates that it has good ability of the electron transfer thereby acts as good corrosion inhibitor as compared to the benzimidazole derivation in the literature [53]. Based on the values of E_{HOMO} and E_{HOMO}, global hardness (η) and softness (σ) values were also derived for MTB. The high value of σ is related with high reactivity; electron donating ability, adsorption tendency and inhibition efficiency and converse is true for η [54–56]. These results suggested that MTB has a good reactive ability and relatively good potent corrosion inhibitors. The low value of dipole moment (2.73 Debye) as compared to the literature [53] suggests that MTB has a good tendency of the polarization thereby acts as good adsorbate on the steel surface. Generally, the compound electron-donating capacity if the back-donation energy less than zero ($\Delta E_{Back\ Donation} < 0$) [62].

According to the results of Table 5, back-donation energy ($\Delta E_{B.D}$) of MTB was less than zero ($\Delta E_{B.D} < 0$), which indicated that the charge transfer from the metal surface to the inhibitor, followed by a back-donation from the inhibitor, was the energetically preferable procedure.

The optimized, HOMO and LUMO frontier molecular orbital pictures of MTB is presented in fig. 7. From this figure it can be seen that HOMO forms of MTB molecules are located over one ring (red) while on the second (bleu) mainly LUMO is located. This observation suggests that the first ring acts as electron donor while the second ring acts as electron acceptor during metal-inhibitor interactions. The Mulliken Atomic Charge (MAC) and ESP surface, as shown in fig. 7, are method to see the electron density visibly. The red (negative) fragments of the MEP represent the sites for nucleophilic attack while blue (positive) fragments denote the sites for electrophilic attack. On the basic of above discussion, it can be concluded that DFT study provide good support to the experimental results and findings.

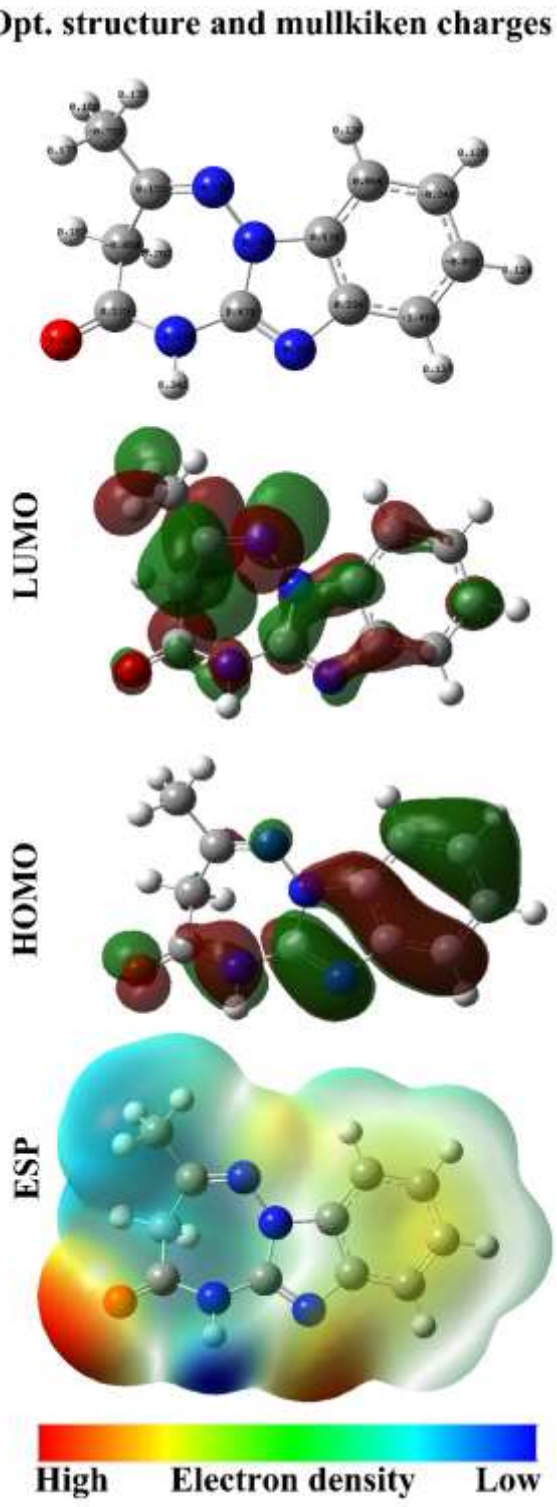

Figure 7: HOMO, LUMO and ESP surfaces of MTB inhibitor and their optimized structure with Mullikan atomic charge (MAC).

5. Conclusions

The 3H-2- Methyl-1,2,4- Triazepino [2,3-a] Benzimidazole-4(5h)-one (MTB) have shown good inhibiting properties for iron corrosion in 1M HCl. The Results obtained from potentiodynamic

polarization indicated that the inhibition efficiency increased with the increasing the MTB concentration and reached to 93%, and besides the MTB act as mixed-type inhibitors. The adsorption of MTB is a spontaneous process and obeys Langmuir adsorption isotherm. The adsorption and thermodynamic parameter (ΔG_{ads}, ΔH_{ads} and E_a) indicate that the adsorption of MTB onto steel surface involves two types of interaction chemical and physical adsorption. DFT studies of natural MTB molecule provide good support with the experimental results and established that MTB interact strongly onto steel surface.

References

[1] H. Keles, M. Keles. Mater. Chem. Phys., 112 (2008) 173–179.
[2] D. Choi, S.You, J. Kim, Mater. Sci. Eng., 335 (2002) 228.
[3] L. John Berchmans, V. Sivan, S. Venkata Krishna Iyer, Mater. Chem. Phys 98 (2006) 395–400.
[4] X.H. Li, G.N. Mu, Appl. Surf. Sci. 252 (2005) 1254–1265.
[5] R. Solmaz, G. Kardas, B. Yazicl, M. Erbil, Colloids Surf. A: Physicochem. Eng. Aspects, 312 (2008) 7–17.
[6] A.Y. El-Etre, M. Abdallah. Corros. Sci., 42 (2000) 731.
[7] H. Saufi, A. Al Maofari, A. El Yadini, L. Eddaif, H. Harhar, S.Gharby, S. El Hajjaji. J. Mater. Environ. Sci., 6:7 (2015) 1845.
[8] J.P. Silvestre, N.Q. Dao, Y. Leroux. Heteroatom Chem., 12 (2001) 73.
[9] S. El Hajjaji, A. Lgamri, H. Abou El Makarim, A. Ben Bachir, A. Guenbour, L. Aries. Prog. Org. Coat., 48 (2003) 63.
[10] M.A. Quraishi, K. Hariom, Mater. Chem. Phys. 78 (2002) 18–21.
[11] A. Al Maofari, M. Mousaddak, A. Hakiki, Y. Suleiman, S. Gamouh, S. Zaydoun, S. El Hajjaji. CTAIJ, 6:2 (2011) 73.
[12] L. Elkadi, B. Mernari, M. Traisnel, F. Bentiss, M. Lagrenee, Corros. Sci. 42 (2000) 703–719.
[13] J.Z. Ai, X.P. Guo, J.E. Qu, Z.Y. Chen, J.S. Zheng, Colloids Surf. A: Physicochem. Eng. Aspects 281 (2006) 147–155.
[14] M. Benmessaoud, A. Al Maofari, Y. Nasser Otaifah, N. Labjar, M. Serghini Idrissi, D. Bartout, S. El Hajjaji. JMES, 8 (11), (2017), 4057-4067
[15] E. McCafferty, Corrosion Control by Coatings, H. Leidheiser editor, Science Press, Princeton, N.J., 279 (1979).
[16] A. Al Maofari, G. Ezznaydy, Y. Idouli, F. Guédira, S. Zaydoun, N.Labjar, S. El Hajjaji. Mater. Environ. Sci. 5 (S1) (2014) 2081.
[17] Z. Akounach, A. Al Maofari, A. El Yadini, S. Douche, M. Benmessaoud, B. Ouaki, M. Damej and S. El Hajjaji. Anal. Bioanal. Electrochem., Vol. 10, No. 11, (2018) 1506-1524.
[18] Z. Wahbi, A. Guenbour, H. Abou El Makarim, A. Ben Bachir, S. El Hajjaji, Progress in Organic Coatings 60 (2007) 224–227.
[19] A.A. Al-Sarawya, A.S. Foudab, W.A. Shehab El-Dein, Desalination, 229 (2008) 279–293.
[20] A.S. Fouda, A.A. Al-Sarawy, E.E. El-Katori, Desalination, 201 (2006) 1–13.
[21] A.Y. Musa, A.A.H. Kadhum, A.B. Mohamad, M.S. Takriff, A.R. Daud, S.K. Kamarudin, Corros. Sci., 52 (2010) 526–533.
[22] F. Bentiss, M. Traisnel, M. Lagrenee, Corros. Sci., 42 (2000) 127–146.
[23] Roland T. Loto, OlukeyeTobilola. Journal of King Saud University – Engineering Sciences, xxx (2016) xxx–xxx.

[24] A. Tazouti, M. Galai, R. Touir, M. EbnTouhami, A. Zarrouk, Y. Ramli, M. Saraçoğlu, S. Kaya,F. Kandemirli, C. Kaya. Journal of Molecular Liquids 221 (2016) 815–832
[25] M.E. Belghiti, Y. Karzazi, A. Dafali, I.B. Obot, E.E. Ebenso, K.M. Emrane, I. Bahadur, B. Hammouti, F. Bentiss. Journal of Molecular Liquids 216 (2016) 874–886
[26] M. Christov, A. Popova, Corros. Sci. 46 (2004) 1613–1620.
[27] S.A. Soliman, M.S. Metwally, S.R. Selim, M.A. Bedair, M. A. Abbas. Journal of Industrial and Engineering Chemistry, xxx (2014) xxx–xxx.
[28] J. Saranya, M. Sowmiya c, P. Sounthari, K.Parameswari, S. Chitra, K. Senthilkumar. Journal of Molecular Liquids, 216 (2016) 42–52.
[29] A. Popova. Corros. Sci, 49 (2007) 2144–2158.
[30] Priyanka Singh, M.A. Quraishi.Measurement, 86 (2016) 114–124.
[31] G. Karthik, M. Sundaravadivelu. Egyptian Journal of Petroleum. 25 (2016) 183–191
[32] I. Ahamad, M.A. Quraishi, Corros. Sci, 52 (2010) 651–656.
[33] M. Errili, A. Al Maofari, K. Tassaoui, M. Damej, Z. Lakbaibi, A. Et-Tahir, S. El Hajjaji and M. Benmessaoud. Int. J. Corros. Scale Inhib., 12:2 (2023) 458–476
[34] A. Ghanbari, M.M. Attar, M. Mahdavian. Materials Chemistry and Physics, 124 (2010) 1205–1209
[35] O.K. Abiola. Corros. Sci., 48:10 (2006) 3078.
[36] Z. Akounach, A. Al Maofari, M. Damej, S. El Hajjaji, A. Berisha, V. Mehmeti, N. Labjar, M. Bamaarouf and M. Benmessaoud. Int. J. Corros. Scale Inhib, 11:1 (2022) 402–424
[37] E.E. Oguzie, Corros. Sci., 49:3 (2007) 1527.
[38] M.N.H. Moussa, A.A. El-Far, A.A. El-Shafei, Mater. Chem. Phys., 105 (2007) 105.
[39] K.F. Khaled, Mater. Chem. Phys., 112 (2008) 104–111.
[40] E.E. Oguzie, Corros. Sci., 49 (3) (2007) 1527.
[41] G. Aziate, A. El Yadini, H. Saufi, A. Al Maofari, A. Benhmama, H. Harhar, S. Gharby, S. El Hajjaji. J. Mater. Environ. Sci., 6:7 (2015) 1877-1884
[42] A.Y. El-Etre. Mater. Chem. Phys., 108 (2:3) (2008) 278.
[43] H. Keles, M. Keles, I. Dehri, O. Serindag, Mater. Chem. Phys., 112 (2008) 173–179.
[44] M. Behpour, S.M. Ghoreishi, N. Soltani, M. Salavati-Niasari, M. Hamadanian, A. Gandomi, Corros. Sci., 50 (2008) 2172–2181.
[45] M.A. Migahed, I.F. Nassar, Electrochimica Acta, 53 (2008) 2877–2882.
[44]R. Solmaz, G. Kardas M. Çulha, B. Yazici, M. Erbil, Electrochimica Acta, 53 (2008) 5941-5952.
[46] GülsenAvci, Colloids and Surfaces A: Physicochemical and Engineering Aspects 317:730 (2008).
[47] F. Bentiss, M. Lebrini, M. Lagrenee, Corrosion Science, 47 (2005) 2915–2931.
[48] A. Al Maofari, F. Guedira, M. Benmessaoud, B. Ouaki, S. El Hajjaji. Albaydha University Journal, 4:03, (2022), 204-213.
[49] A. Al Maofari, S. Douch, M. Benmessaoud, B. Ouaki, M. Mosaddak and S. EL Hajjaji. Portugaliae Electrochimica Acta, 39:1 (2021) 21-35.
[50] A. Eh. Noor, A. H. Al-Moubaraki, Materials Chemistry and Physics, 110 (2008) 145-154.
[51] L. Larabi, Y. Harek, O. Benali, S. Ghalem. Progress in Organic Coatings, 54 (2005) 256-262.
[52] X. Li, S. Deng, H. Fu, G. Mu. Corrosion Science, 51 (2009) 620-634.
[53] Chandrabhan Verma, J. Haque, Eno E. Ebenso, M.A. Quraishi. Results in Physics, 9 (2018) 100–112.

[54] A. Kadhim, A.K. Al-Okbi, D.M. Jamil, A. Qussay, A.A. Al-Amiery, T.S. Gaaz, A.A.H. Kadhum, A.B. Mohamad, M.H. Nassir. Results Phys., 7 (2017) 4013.
[55] A. Zarrouk, B. Hammouti, A. Dafali, M. Bouachrine, H. Zarrok, S. Boukhris, S.S. Al-Deyab. J Saudi Chem Soc.,18 (2014) 450.
[56] Mosaad R. Mlahi, Elsayed M. Afsah, Amr Negm and Mohsen M. Mostafa. Appl. Organometal. Chem., (2015) DOI 10.1002/aoc.3265.
[56] Y.U. Abdulbasit, B. U. Abdullahi and U. Bishir. Mor. J. Chem., 14:2 (2023) 282-299.
[57] L. El Ghayati, A. Batah, M. Belkhaouda, L. Bammou, R. Salghi, A. Saber, A. Chetouani, M. L. Taha, E. M. Essassi. Mor. J. Chem., 7:3 (2019) 567-579.
[58] N. Obi-Egbedi, I. Obot, M.I. El-Khaiary. J Mol Struct., 1002 (2011) 86–96.
[59] Hamdouch A., Anejjar A., Bijla L., Gharby S., Asdadi A., Chebli B., Salghi R., Idrissi Hassani L. M. Mor. J. Chem., 14:1 (2023) 105-118.
[60] Shaimaa B. Al-Baghdadi, Fanar G. Hashim, Ahmed Q. Salam, Talib K. Abed, Tayser Sumer Gaaz. Ahmed A. Al-Amiery, Abdul Amir H. Kadhum, Khalid S. Reda, Wahab K. Ahmed. Results in Physics, 8 (2018) 1178–1184.
[61] Hasna Belcadi, Anas Chraka, Soukaina El Amrani, Ihssane Raissouni, Abderrahman Moukhles, Said Zantar, Larbi Toukour, Ahmed Ibn Mansour. Journal of Bio- and Tribo-Corrosion, 9:50 (2023) 5-28.